JOURNAL OF SPACECRAFT AND ROCKETS
Vol. 30, No. 4, July–August 1993

High Velocity Atomic Oxygen/Surface Accommodation Studies

R. H. Krech,* M. J. Gauthier,† and G. E. Caledonia‡
Physical Sciences Inc., Andover, Massachusetts 01810

This paper provides the first laboratory evaluation of the energy accommodation coefficients of 8 km/s oxygen atoms on selected materials. Preliminary measurements have been provided for three materials at normal incidence. Neglecting chemical energy, the accommodation coefficients for nickel, gold, and reaction cured glass are all approximately 0.6 ± 50%.

Nomenclature

C_p = specific heat of sample, ergs g^{-1}
I = oxygen atom beam average energy flux, ergs-cm^{-2} s^{-1}
k = thermal conductivity of sample, erg cm^{-2} s^{-1} K^{-1}
ℓ = thickness of sample, cm
T = temperature, K
T_0 = initial temperature, K
t = time, s
α = energy accommodation coefficient
ΔT = temperature increase, $T - T_0$, K
ϵ = total sample emissivity
σ = Stefan-Boltzmann constant = 5.67×10^{-12}, W/K^4-cm^2

Subscript

0 = initial time

I. Introduction

THE lack of experimental data on the energy and momentum accommodation coefficients of high-velocity air species with aerospace materials has become a critical issue with the advent of experiments such as the NASA Aeroassist Flight Experiment and developmental projects such as the National Aerospace Plane (NASP) and the Aeroassisted Orbital Transfer Vehicle (AOTV), all of which will operate at hypersonic speed in rarefied flows. In this work we describe preliminary measurements of the energy accommodation coefficient of 8 km/s oxygen atoms impacting selected surfaces. These measurements were performed using a recently developed fast atom source[1-3] which employs laser-induced gas breakdown to provide a high flux of atomic oxygen and/or mixtures of N/N_2 in the velocity range of 4–12 km/s.

Hurlbut[4] has recently reviewed our understanding of the interactions between gas molecules and solid surfaces at high velocities in rarefied flow and has further addressed the state of gas/surface scattering models to satellite applications.[5] High-velocity energy and momentum accommodation coefficients are fundamental to analyses involving free molecular and transition flow around hypersonic vehicles. In particular, the NASP and the AOTV will operate in rarefied flow regimes corresponding to the transition region between the free molecular and continuum limits. This flow regime is not well simulated in presently available hypersonic flow facilities, and thus performance predictions (heat transfer, lift/drag, etc.) and system design must rely on a combination of theoretical models and previous flight experience. The direct simulation Monte Carlo technique seems particularly appropriate for such analysis.[6-8] Energy and momentum accommodation coefficients are required inputs to this model.

These coefficients will be both velocity and species dependent and will vary with collision angle, material, and surface temperature. In the case of interaction with free radicals, such as O and N, surface-catalyzed recombination reactions can occur producing molecular species and releasing heat to the surface, as discussed in Ref. 9. The product molecules, however, may be formed internally excited, i.e., electronically, vibrationally, and rotationally, and thus the surface may not receive the full energy potential of the reaction.[10-13] Naturally, the manifold of such surface-catalyzed reactions can effect the degree of momentum transfer to the surface. Even nonreactive species can exhibit significant variations in momentum transfer, which are critical for specification of lift/drag behavior.

Prior to the present study, there had been no laboratory measurements of oxygen atom energy/momentum accommodation coefficients at orbital velocities.[4] Cross and Cremers[14] and Cross et al.[15] have, however, shown that approximately one-half the kinetic energy is accommodated when 4.4 km/s oxygen atoms strike a NiO surface. As discussed further in the text, we have now provided preliminary measurements of the energy accommodation coefficient for 8 km/s oxygen atoms impinging three materials: reaction cured glass (RCG), nickel, and gold. These measurements were performed with our fast atom source through monitoring sample heating via infrared (IR) pyrometry.

The details of our work are provided as follows. Section II provides an overview of the phenomena studied, including an analytical description of the accommodation coefficient evaluation. Section III provides an overview of the experimental technique, data base, and interpretation, and Sec. IV presents a summary of our results with recommendations for additional effort.

II. Phenomenological Overview

There are four possible general interactions that can occur when a fast oxygen atom strikes a clean surface: 1) a fast atom scatters off the surface without chemical reaction with or without momentum accommodation; 2) a fast O-atom recombines with another on the surface and then either adsorbs to or migrates from the surface; 3) a fast O-atom reacts with a surface forming an oxide which migrates from the surface; and 4) the fast atom oxidizes the surface or diffuses into the material producing a solid-phase oxide with perhaps an intermediate species leaving the surface (surface spalling can occur in this situation).

In case 1, there can be kinetic energy exchange with the surface, with directly relatable momentum exchange. In the remaining cases, there will definitely be kinetic energy exchange, momentum accommodation, and some chemical energy transfer. The partitioning among these processes must be

Received June 5, 1991; presented as Paper 91-1339 at the AIAA/ASME 5th Joint Thermophysics and Heat Transfer Conference, Seattle, WA, June 18–20, 1991; revision received Nov. 15, 1991; accepted for publication Jan. 2, 1992.

*Principal Scientist, 20 New England Business Center.
†Senior Engineer, 20 New England Business Center.
‡President, 20 New England Business Center. Senior Member AIAA.

understood to specify heat transfer, lift, and drag on hypersonic vehicles in rarefied flows. Four different diagnostics are required to totally unravel these effects: measurements of energy and momentum accommodation, identification of species leaving the surface, and surface characterization, i.e., mass loss, oxidation, etc.

The primary object of the present work was to measure the total energy accommodation coefficient by monitoring the temperature increase on a thermally isolated sample irradiated by PSI's (Physical Sciences Inc.) pulsed fast O-atom beam.[1-3] The experimental procedure involved continued irradiation of the front surface of a thin sample with the fast O-beam; this produced surface heating through accommodation that was monitored at the sample back surface with optical pyrometry. The details of the O-atom source and sample measurement techniques are provided in the next section; a schematic of the phenomenology involved is presented in Fig. 1. As will be seen, the fast atom source is pulsed, however, the characteristic sample heating times are quite long compared to the time for sample temperature equilibration, and thus the heating may be treated as if the result of continuous irradiation.

An 8 km/s oxygen atom carries a kinetic energy of ~ 5 eV and a chemical enthalpy of an additional 2.5 eV; the thermal enthalpy of the atom C_pT is negligible compared to these former two quantities. On striking the surface, the atom will provide some fraction of this energy to the surface in the form of sensible heat. Since in the present case transfer of thermal energy from the surface to the gas is negligible, this fraction is by definition the energy accommodation coefficient.[16] Note that it can have contributions due both to momentum transfer and chemical reaction. The energy transmitted to the sample surface will be conducted throughout the target, the characteristic conduction time being τ_c, where

$$\tau_c = \rho C_p \ell / k$$

where axial conduction is not considered since the target is assumed to be uniformly irradiated.

Since the sample is in vacuum and thermally isolated, the dominant heat loss mechanism is radiative transfer, as determined by the sample temperature and the material emissivity. The oxygen atom pulses used in our study have temporal widths on the order of 30 μs. Thus if one monitored the front surface temperature with ~ 1 μs temporal resolution one could monitor the whole process of accommodation followed by thermal conduction and radiative cooling. We were not able to accomplish this in the present effort and instead used a diagnostic that could monitor back surface temperature at 20 ms temporal resolution (see Sec. III). This latter diagnostic was quite useful since with continued target irradiation the back surface temperature must ultimately reach a steady temperature which reflects a balance between energy accommodation and radiation cooling.

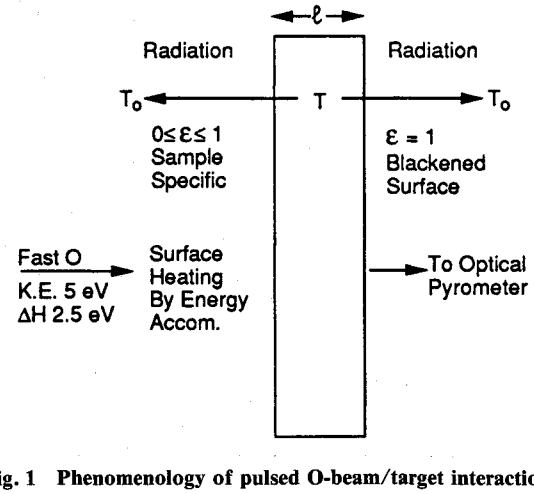

Fig. 1 Phenomenology of pulsed O-beam/target interaction.

A simple expression for the back surface temperature history can be defined under the assumptions that the conduction time is short compared to the O-atom interpulse time, which is short compared to the radiative cooling time. These assumptions are appropriate for the present experiments. In this limit, the target can be taken as isothermal and the O-atom source can be assumed to be continuous, having an average energy intensity defined as the product of the total O-atom energy per pulse times the O-atom source repetition frequency, i.e., the average energy intensity is defined as the product of the number of oxygen atoms/cm^2/pulse, the energy per oxygen atom (~ 7.5 eV at $v = 8$ km/s) and the repetition frequency.

In this limit, the general heat balance equation for a sample uniformly irradiated on one side with an O-atom beam of average energy flux I with radiation as the only loss is

$$\rho C_p \ell \frac{dT}{dt} = \alpha I - (1+\epsilon)\sigma(T^4 - T_0^4) \tag{1}$$

We assume that the sample is a grey body with emissivity ϵ on the irradiated side and unity on the blackened side (see Fig. 1).

In steady state

$$\alpha I = (1+\epsilon)\sigma(T_{SS}^4 - T_0^4)$$

where the subscript SS refers to steady state. For small temperature increases, $T = T_0 + \Delta T$, Eq. (1) reduces to

$$\alpha = [4(1+\epsilon)\sigma T_0^3 \Delta T_{SS}]/I \tag{2}$$

independent of all material properties, with the exception of emissivity. For small ΔT, Eq. (1) can be rewritten as

$$\frac{d\Delta T}{dt} = (\rho C_p \ell)^{-1}[\alpha I - 4(1+\epsilon)\sigma T_0^3 \Delta T]$$

which has the general solution

$$\Delta T = \frac{\alpha I}{4(1+\epsilon)\sigma T_0^3}\{1 - \exp[-4(1+\epsilon)\sigma T_0^3 t/(\rho C_p \ell)]\} \tag{3}$$

which, of course, asymptotes to the steady solution of Eq. (2) as $t \to \infty$.

The important additional feature in Eq. (3) is that the characteristic time to approach within $(1 - e^{-1})$ of steady state is

$$\tau = \rho C_p \ell / [4(1+\epsilon)\sigma T_0^3] \tag{4}$$

independent of α.

Furthermore, when the O-beam is terminated, Eq. (1) reduces to

$$\rho C_p \ell \frac{d\Delta T}{dt} = 4(1+\epsilon)\epsilon\sigma T_0^3 \Delta T$$

where

$$\Delta T = \Delta T_{SS} \exp[-4(1+\epsilon)\sigma T_0^3 t/\rho C_p \ell] \tag{5}$$

with, of course, the same time constant τ.

Although, as described in Sec. III, the full temporal temperature history was measured, the two key quantities used in the present analysis are ΔT_{SS} and τ. Note that τ is just a function of the material properties and thus its measurement assures that the phenomenology is understood. Alternately, ΔT_{SS} is independent of the material properties with the exception of emissivity. This simple analysis was validated using a detailed computer model that evaluated the pulse-by-pulse two-dimensional temperature histories for the materials tested.

The situation is actually more complicated than that portrayed so far in that there are additional energy sources that contribute to the target heating and thus should be included on

the right-hand side of Eq. (1). As discussed in the next section, the dominant one of these is the absorption of scattered light from the laser pulse used to create the oxygen atom beam. There may also be some small contribution due to plasma radiation. The experimental solution to this problem was to place a shutter in front of the sample, which allowed transmission of radiation but not the oxygen atom beam. The sample temperature history in this instance was used to evaluate the intensity of the radiative heating source. This data was then used as a correction to the temperature profile measured in the presence of the full beam to evaluate the contribution due to oxygen atom heating.

We note that the laser pulse used to form the fast O-beam has a time duration of 2.5 μs whereas the O-atom pulse has an $\sim$ 30 μs duration. Thus, if we had used a front surface temperature monitor with microsecond temporal resolution, the two effects would have been readily delineated. Such a diagnostic will be used in future measurements.

III. Experimental Technique, Data Base, and Interpretation

A thermally isolated sample suspended in a high vacuum chamber will establish an equilibrium temperature equal to the chamber temperature solely by radiative energy transfer which is independent of the emissive properties of the chamber and the sample. If this sample is then exposed to a suprathermal molecular flow, some of the beam translational energy will be lost to the sample by beam-surface collisions. The accommodated translational energy will raise the temperature of the sample to a new, higher equilibrium value determined solely by the radiative properties of the sample and the chamber walls. This new temperature is dependent on the emissivity of the sample. Since by design energy can be lost only through radiation, samples with low emissivities will be hotter than samples with unit emissivity when irradiated with the same flux. If the radiative properties of the sample are known (or measured), and the beam flux and energy are measured, then the thermal energy accommodation coefficient can be readily determined by measuring the sample temperature.

The use of classical surface contact thermometry will yield inaccurate temperature measurements if the probe has significant thermal conductivity and/or the sample has low thermal conductivity. Temperature measurement techniques employing noncontact optical pyrometry eliminate these inaccuracies and permit very precise temperature measurements. The most accurate temperature measurements are obtained when the sample emissivity is unity, therefore we painted the back of the samples with black paint. Measurement of the equilibrium rear surface temperature of a sample painted black to insure an emissivity of unity can yield precision of $\pm$ 0.05 K, which approximately translates to a 2% uncertainty in the accommodation coefficient measurement for a sample temperature rise of 3 K. The actual total sample emissivity can either be measured directly by infrared spectroscopy, or by observing the radiative cooling rate of a sample heated in vacuum, as discussed in Sec. II. The latter approach has sufficient accuracy and is much simpler than the former method and therefore was chosen for the present measurements.

As mentioned earlier, there is an additional source of sample heating in the experiment in addition to the atomic oxygen accommodation. The oxygen beam is created through CO_2 laser-induced O_2 gas breakdown within a hypersonic expansion nozzle.[1] The absorption of the laser energy used to generate the atomic oxygen beam is not 100% efficient, and some fraction of the laser energy is scattered out from the nozzle back into the chamber, raising the temperature of both the chamber and the samples. The sample temperature increase is a function of both the scattered radiation intensity, and the absorptivity of the front surface of the sample at 10.6 μm, the laser wavelength. This additional source of heating must be accounted for in the test procedure and analysis, and requires an additional temperature measurement. All of the samples in these experiments have constant IR emissivities. Since by definition at a given wavelength the emissivity equals the absorptivity, the average IR emissivity can be used as the 10.6 μm absorptivity.

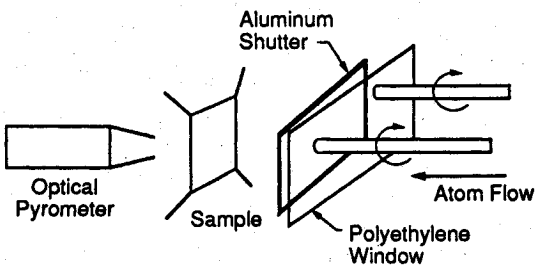

Fig. 2 Experimental schematic.

A schematic drawing of the experimental measurement system is shown as Fig. 2. The sample is positioned to intercept the atomic oxygen beam downstream of the nozzle. The optical pyrometer is placed behind the sample. There are two shutters that can be lowered between the samples and the O-beam to permit measurement of the background radiative load and scattered laser radiation heating.

The first of these is an aluminum plate which can be positioned in front of the sample with the source operating so as to allow the chamber to reach an equilibrium temperature with the source in operation. In this instance, the background temperature is measured with no atoms or scattered laser radiation on the target. The sample heating due to the scattered laser radiation is measured by replacing the aluminum shutter with a polyethylene film. (The film transmits 85% at 10.6 μm.) This film transmits the CO_2 laser radiation (and any plasma radiation) while stopping the O-atom beam. The equilibrium temperature rise due to the laser irradiation of the samples can be measured and corrected to a 100% transmission level. With both shutters removed the temperature rise due to both the atomic oxygen accommodation and scattered laser (and plasma) radiative heating is recorded. By subtraction of the two measurements, the temperature rise due to atomic oxygen accommodation can be calculated.

The translational energy accommodation coefficient measurements were conducted in the PSI FAST-2 (Fast Atom Sample Tester) device. The operating principles and characterization of the O-beam source are provided in Refs. 1-3. The FAST-2 device generates a large area (30–2000 cm^2), high flux (to $>10^{16}$ atoms/cm^2-s) pulsed atomic oxygen beam which is readily tunable from below 2 eV to as high as 14 eV. For the accommodation coefficient measurements, the beam energy was 5 eV (7.8 km/s) with a beam pulse half-width of $\sim$ 30 μs, and only normal incidence was evaluated. The beam velocity spread is $\pm$ 15%. The beam ion concentration is $<$1%, an unimportant level for the present measurements. The beam is $>$80% oxygen atoms as determined by mass spectrometry. We believe the actual percentage is larger since surface recombination of O-atoms occurs within the mass spectrometer.

Three different materials were studied: RCG, nickel, and gold. The RCG samples were prepared by the NASA Johnson Space Center by vapor depositing a 0.5-mm-thick layer of RCG on 1.5-mm-thick, 2.5-cm-diam fused silica substrates. The nickel samples were cut from 0.127-mm-thick 2.5-cm nominal diameter 99.9% pure nickel sheet. The nickel was not treated to remove surface oxides. The gold samples were fabricated by electroplating gold onto nickel samples. The rear surfaces of all samples were spray painted with a thin layer of Krylon Ultra Flat Black paint to insure a 99 + % infrared emissivity for maximum temperature sensitivity. No special cleaning procedures were adopted for the samples prior to irradiation and the nickel sample was undoubtedly surface oxidized.

Sample temperatures were measured optically with an OMEGA Model OS-604 pyrometer. These pyrometers employ

an 8–14 μm sensor with a 1:3 field of view and have digital display units with a 1.8 mV/K recorder output. These devices are not specifically for vacuum application, but are readily modified by adding plugs to the sensor cable to permit sensor installation within the chamber, while positioning the readout outside the chamber. (Modular telephone jacks, plugs, and 12-ft long cables were used for the adaptation and the cables were potted in epoxy on a vacuum feedthrough.) After modification, the sensor calibration was verified by pointing the sensor at a black painted can filled with ice water and boiling water.

The three samples were positioned 25 cm downstream from the nozzle throat on a thermal isolation mount, which allowed translation of the samples perpendicular to the flow centerline. Thermal isolation was achieved by gluing three 0.25-mm stainless-steel wires to the metal samples and attaching these wires to 4-40 nylon screws on the sample mount. The RCG sample was held radially in position by three 4-40 nylon screws in compression on the outer diameter.

The optical pyrometer sensor head was mounted inside the vacuum chamber approximately 3.75 cm below flow centerline and approximately 1 to 2 cm behind the sample holder. The field of view was approximately 1.5 cm in diameter centered on the back of the selected sample. The sample holder is translated perpendicular to the flow to enable the observation of the individual samples. The output of the readout was recorded on a chart recorder operating at 20 cm/h scan rate and 50-mV full scale sensitivity (280–311 K temperature scale). The readings could be interpolated to ± 0.05 K.

Prior to each measurement the fast O-beam was operated for approximately 1 h to permit: 1) the source to stabilize prior to data recording, with the aluminum shutter plasma in front of the samples, and 2) to record the background thermal temperature. The aluminum shutter is then removed and the polyethylene shutter is positioned in front of the sample. The temperature is then recorded for approximately 1.5 h until the equilibrium laser heating temperature is established. The polyethylene shutter is then removed and the temperature is recorded for approximately 0.5 h until the equilibrium accommodation and laser heating temperature is established. This sequence was repeated several times on a single measurement to insure reproducibility. At the end of the measurement the system is shut down; the radiative cooling rate is recorded to insure that the sample is indeed thermally isolated.

It should be noted that these measurements were not made under ultrahigh vacuum conditions. The background pressure was maintained below 10^{-5} Torr, sufficiently low so that collisions with the background gas do not slow down the fast pulse of oxygen atoms. As will be seen, the average O-beam flux is of the same order as the random flux of background molecules striking the surface, however, the instantaneous O-beam flux is much higher. We find that samples in our system are scoured clean by the fast oxygen beam within the first few seconds of beam operation. Thus, we believe that surface contamination effects do not impact our observations.

The source was operated at 3-Hz pulse rate for these measurements and the typical average flux was between $2\text{–}7 \times 10^{15}$ atoms/cm^2-s. The atomic oxygen flux is determined by positioning a Kapton H witness sample at the same axial and radial distance from the nozzle throat as the sample. The Kapton H reactivity with atomic oxygen is well documented, and the accepted mass erosion rate is 4.2×10^{-24} g/atom at 5 eV.[17] This Kapton H sample is placed in the chamber at the beginning of a test sequence and removed after the test is completed. The average pulse fluence is calculated by measuring the mass loss per unit area of the sample and dividing by the number of pulses of the source. The average flux density is determined by multiplying the fluence per pulse by the pulse rate of the source. During a typical test sequence, a 6.3-cm^2 Kapton H sample lost between 1 and 4 mg. This mass loss can be measured quite accurately with a Cahn Model 31 microbalance, which has a precision of 1 μg. (Of course, care must be taken to avoid moisture pickup in the Kapton H sample prior to measurement.) Thus, the accuracy of the flux determination is limited by the accuracy of the mass erosion rate used and the steadiness of the source over time. The combined effects should yield an average flux value to significantly better than a factor of two. This accuracy will be improved in future measurements by use of calorimetric techniques.

The O-atom flux levels were chosen to ensure sufficient sample heating while maintaining the true molecular limit. To do this we require that the line density of oxygen atoms/cm^2 in a single pulse be low enough to allow only minimal interactions between incident atoms and scattered or absorbed atoms. During the measurements, the line density per pulse was varied between 0.7 and 2.3×10^{15} cm^2. An atomic surface monolayer would exhibit a line density of $\sim 2 \times 10^{15}$ cm^2. Thus, even at the highest fluxes employed, beam-adsorbate interactions could only dominate if all of the incident O-atoms stuck to the surface for a period longer than the pulse duration, an observation not borne out by the data. Similar arguments prevail for incident/scattered atom collisions.

A typical temperature record for gold is shown in Fig. 3. In this trace, the first plateau on the left corresponds to the equilibrium sample temperature with the source operating and the sample shuttered by the aluminum plate. The next plateau represents the temperature rise due to scattered radiation with the polyethylene shutter in position. The highest plateau indicates the temperature rise due to both radiative and accommodation heating of the sample. On the far right is the radiative cooling curve of the sample with the beam off, which is used to confirm our emissivity and thermal isolation criteria. Three data sets were taken, with total flux and initial target temperatures as the primary variables. In all cases the observed target cooling on beam termination was accurately reflected by Eq. (5), validating the thermal isolation of the target materials.

Typically, the radiative heating of the metallic samples was between 1 and 2 K, with the accommodation heating providing between 2 and 3 K heating above that. The 10.6-μm absorptivity of the metals was evaluated as $<10\%$. The radiative heating of the RCG was large in comparison to the metals, reflecting its higher absorptivity at 10.6 μm. The radiative heating raised the RCG temperatures between 7 and 16 K, whereas the combined additional radiative and accommodation heating was only 1.5 to 4.5 K above that.

A purely statistical analysis of the data is presented in Table 1 with the standard deviations reflecting only the scatter in the measurements. The total energy accommodation coefficients for all three materials are similar, and for practical purposes are approximately 0.4. The degree of surface recombination remains unspecified in the measurements. We note that the recombination coefficient is a strong function of pressure. For example, the recombination coefficient for thermal oxygen atoms on gold is <0.01 at moderate pressures,[9] ~ 1 Torr, but has been reported to be 0.27 at pressures $<10^{-7}$ Torr.[18] There are no laboratory measurements of heterogeneous oxygen atom recombination at orbital velocity impact although a complex analysis of the OGO-6 neutral mass spectrometer

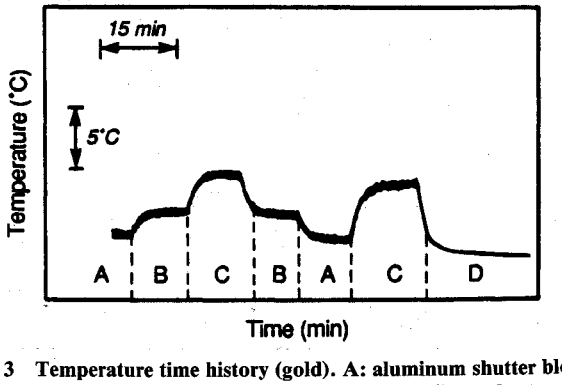

Fig. 3 Temperature time history (gold). A: aluminum shutter blocking beam; B: polyethylene shutter blocking beam; C: no shutter; and D: beam termination.

Table 1 Data summary

Material	Total energy accommodation coefficient[a]	Translation energy accommodation coefficient[a]
RCG	0.36 ± 0.08	0.54 ± 0.12
Nickel	0.35 ± 0.06	0.53 ± 0.09
Gold	0.43 ± 0.12	0.64 ± 0.1

[a]Average values of three measurements.

data has been provided.[19] In any event, one can consider the lower limit of no surface recombination. If this assumption were valid, then only the kinetic energy of the system is accommodated, and the kinetic energy accommodation coefficient would be approximately 0.6 for the three materials. (Confirmation of this hypothesis requires an independent measurement of the momentum transfer which will be provided in future studies). Given the scatter in the data and the uncertainty in the fluence calibration, these measurements are uncertain to approximately $\pm 50\%$. Future measurements, employing a beam energy trap, will reduce this uncertainty.

IV. Summary

In summary, the ability to measure energy accommodation coefficients of 8 km/s oxygen atoms on selected materials has been demonstrated. Preliminary measurements have been provided for three materials at normal incidence. These are the first such evaluations performed for high-velocity oxygen atoms. Neglecting chemical energy, the energy accommodation coefficients for nickel, gold, and RCG are all approximately $0.6 \pm 50\%$. This level of accommodation would result in average scattered oxygen atom velocities of ~ 5 km/s.

The present measurements are limited and still have high levels of uncertainty. The key parameters which affect the accuracy of the evaluations are the scattered CO_2 laser light and the absolute calibration of the fast O-beam. The first effect can be minimized by a combination of both reducing the intensity of scattered laser light and providing a fast front surface temperature monitor. The need for an absolute O-beam calibration can be eliminated by monitoring the temperature of a momentum trap, a device which forces total accommodation of the O-beam through multiple internal collisions. A research program is presently being developed to extend this technique to allow careful measurement of the total energy accommodation coefficient and the total and differential momentum transfer coefficients of 8 km/s oxygen atoms on selected surfaces.

Acknowledgements

This research was supported by the NASA Johnson Space Center under Contract NAS7-18326. The contract monitor was S. Fitzgerald. The authors acknowledge valuable discussions with A. Gelb, T. Rawlins, and W. Marinelli of Physical Sciences Inc., and useful suggestions from the manuscript referees.

References

[1]Caledonia, G. E., Krech, R. H., and Green, B. D., "A High Flux Source of Energetic Oxygen Atoms for Material Degradation Studies," *AIAA Journal,* Vol. 25, No. 1, 1987, pp. 59–63.

[2]Caledonia, G. E., "Laboratory Simulations of Energetic Atom Interactions Occurring in Low Earth Orbit," *Rarefied Gas Dynamics: Space Related Studies,* edited by E. P. Muntz, D. P. Weaver, and D. H. Campbell, Vol. 116, Progress in Astronautics and Aeronautics, AIAA, Washington, DC, 1989, pp. 129–142.

[3]Krech, R. H., and Caledonia, G. E., "Laser Supported Detonation Wave Source of Atomic Oxygen for Aerospace Material Testing," *Current Topics in Shock Waves,* edited by Y. W. Kim, Vol. 208, AIP Conference Proceedings, Bethlehem, PA, 1989, pp. 377–382.

[4]Hurlbut, F. C., "Particle Surface Interaction in the Orbital Context: A Survey," *Rarefied Gas Dynamics: Space Related Studies,* edited by E. P. Muntz, D. P. Weaver, and D. H. Campbell, Vol. 116, Progress in Astronautics and Aeronautics, AIAA, Washington, DC, 1989, pp. 419–450.

[5]Hurlbut, F. C., "Gas/Surface Scatter Models for Satellite Applications," *Thermophysical Aspects of Reentry Flows,* edited by J. N. Moss and C. D. Scott, Vol. 103, Progress in Astronautics and Aeronautics, AIAA, New York, 1986, pp. 97–119.

[6]Moss, J. H., and Scott, C. D. (eds.), *Thermophysical Aspects of Reentry Flows,* Vol. 103, Progress in Astronautics and Aeronautics, AIAA, New York, 1986.

[7]Bartel, T. J., and Hudson, M. L., "Energy Accommodation Modeling of Rarefied Flow Over Reentry Vehicle Geometries Using DSMC," AIAA Paper 89-1879, June 1989.

[8]Moss, J. N., Bird, G. A., and Dogra, V. A., "Non-equilibrium Thermal Radiation for an Aero-assist Flight Experimental Vehicle," AIAA Paper 88-0081, Jan. 1988.

[9]Bamford, C. H., Tipper, C. F. H., and Compton, R. G. (eds.), "Reactions of Solids with Gases," *Chemical Kinetics,* Vol. 21, Elsevier, Oxford, England, 1984, pp. 151–235.

[10]Chu, A-L., Reems, R. R., and Halstead, J., "Surface-Catalyzed Formation of Electronically Excited Nitrogen Dioxide and Oxygen," *Journal of Physical Chemistry,* Vol. 90, No. 3, 1986, pp. 466–471.

[11]Bernasek, S. L., "State-Resolved Dynamics of Chemical Reactions at Surfaces," *Chemical Reviews,* Vol. 87, No. 1, 1987, pp. 91–100.

[12]Sharpless, R. L., Jusinski, L. E., and Slanger, T. G., "Surface Chemistry of Metastable Oxygen. I. Production and Loss of the 4 to 5 eV States," *Journal of Chemical Physics,* Vol. 91, No. 12, 1989, pp. 7936–7946.

[13]Caledonia, G. E., Holtzclaw, K. W., Green, B. D., Krech, R. H., Leone, A., and Swenson, G., "Laboratory Investigation of Shuttle Glow Mechanisms," *Geophysical Research Letters,* Vol. 17, No. 11, Oct. 1990, pp. 1881–1884.

[14]Cross, J. B., and Cremers, D. A., "High Kinetic Energy (1 to 10 eV) Laser Sustained Neutral Atom Beam Source," *Nuclear Instruments and Methods in Physics Research B13,* North Holland Physics Publishing, Amsterdam, 1986, pp. 658–662.

[15]Cross, J. B., Spangler, L. H., Hoffbauer, M. A., and Archuleta, F. A., "High Intensity 5 eV CW Laser Sustained O-Atom Exposure Facility for Material Degradation Studies," *SAMPE Quarterly,* Vol. 18, No. 2, 1987, pp. 41–47.

[16]Sexena, S. C., and Joshi, R. K., "Thermal Accommodation and Adsorption Coefficients of Gases," *CINDAS Data Series on Material Properties,* Vol. II-1, edited by C. Y. Ho, Hemisphere, New York, 1989, pp. 3–13.

[17]Leger, L. J., and Visentine, J. T., "A Consideration of Atomic Oxygen Interactions with the Space Station," *Journal of Spacecraft and Rockets,* Vol. 23, No. 5, 1987, pp. 505–511.

[18]Sjolander, G. W., "Atomic Oxygen Metal Surface Studies as Applied to Mass Spectrometry Measurements of Laser Planetary Atmospheres," *Journal of Geophysical Research,* Vol. 81, No. 22, 1976, pp. 3767–3770.

[19]Hedin, A. F., Hinton, B. B., and Schmitt, G. A., "Role of Gas-Surface Interactions in the Reduction of OGO-6 Neutral Particle Mass Spectrometer Data," *Journal of Geophysical Research,* Vol. 78, No. 22, 1973, pp. 4651–4668.

Gerald T. Chrusciel
Associate Editor